Journal of ELECTRONIC MATERIALS, Vol. 47, No. 5, 2018
https://doi.org/10.1007/s11664-018-6155-3
© 2018 The Minerals, Metals & Materials Society

Temperature-Dependent Electrical Characteristics of Au/Si_3N_4/4H *n*-SiC MIS Diode

F. YIGITEROL,[1] H.H. GÜLLÜ,[2,3] Ö. BAYRAKLI,[3,4,5] and D.E. YILDIZ[1,6,7]

1.—Department of Physics, Hitit University, 19030 Çorum, Turkey. 2.—Centeral Laboratory, Middle East Technical University, 06800 Ankara, Turkey. 3.—Center for Solar Energy Research and Applications, Middle East Technical University, 06800 Ankara, Turkey. 4.—Department of Physics, Middle East Technical University, 06800 Ankara, Turkey. 5.—Department of Physics, Ahi Evran University, 40200 Kırşehir, Turkey. 6.—e-mail: desrayildiz@hitit.edu.tr. 7.—e-mail: desrayildiz@gmail.com

Electrical characteristics of the Au/Si_3N_4/4H n-SiC metal–insulator-semiconductor (MIS) diode were investigated under the temperature, T, interval of 160–400 K using current–voltage (I–V), capacitance–voltage ($C-V$) and conductance–voltage ($G/\omega-V$) measurements. Firstly, the Schottky diode parameters as zero-bias barrier height (Φ_{B0}) and ideality factor (n) were calculated according to the thermionic emission (TE) from forward bias I–V analysis in the whole working T. Experimental results showed that the values of Φ_{B0} were in increasing behavior with increasing T while n values decreased with inverse proportionality in n versus Φ_{B0} plot. Therefore, the non-ideal I–V behavior with inhomogeneous barrier height (BH) formation has been discussed under the assumption of Gaussian distribution (GD). From the GD of BHs, the mean BH was found to be about 1.40 eV with 0.1697 standard deviation and the modified Richardson constant A^* of this diode was obtained as 141.65 A/cm^2 K^2 in good agreement with the literature (the theoretical value of A^* is 137.21 A/cm^2 K^2). The relationship between Φ_{B0} and n showed an abnormal I–V behavior depending on T, and it was modeled by TE theory with GD of BH due to the effect in inhomogeneous BH at the interface. Secondly, according to Cheung's model, series resistance, R_S values were calculated in the T range of 160–400 K and these values were found to decrease with increasing T. Finally, the density of interface states, D_{it} was calculated and the T dependence of energy distribution of D_{it} profiles determined the forward $I-V$ measurements by taking into account the bias dependence of the effective BH, Φ_e and n. D_{it} were also calculated according to the Hill–Coleman method from $C-V$ and $G/\omega-V$ analysis. Furthermore, the variation of D_{it} as a function of frequency, f and T were determined.

Key words: MIS diode, Gaussian distribution, series resistance, surface state

INTRODUCTION

In recent years, wide-band gap semiconductors have been of interest in applications of MIS-type Schottky diodes (SDs).[1–5] In fact, SD is the basic metal-insulator-semiconductor (MIS) device in the technological applications, mainly bipolar integrated circuits.[6,7] Moreover, the SDs play an important role in devices operating at cryogenic temperatures as infrared detectors, thermal imagers, microwave diodes, gates of transistors, and particle detectors.[6–9] The device characteristics of MIS structures are mainly dependent on the semiconductor layer, especially its mechanical and physical properties. Therefore, silicon-carbide (SiC) becomes an attractive material to fabricate the

(Received September 9, 2017; accepted February 16, 2018; published online March 5, 2018)

device structures that can be alternatives to their Si counterparts.[10,11] Compared to Si, this compound semiconductor offers superior properties in terms of dielectric breakdown field strength, saturated electron drift velocity, electron mobility and thermal conductivity.[3,12] With these material properties, SiC-based devices can tolerate high values of breakdown voltage and show low electrical resistivity behavior.[13] Therefore, SiC SD has been of interest due to its potential for use in high-power, high-frequency, and radiation-resistant applications.[14–16] Large band gap characteristics of this compound allow a lower series resistance (R_S) and lower power dissipation under high bias voltages.[10] The availability of high-quality SiC also give an advantage in fabrication steps.[11] In addition to the surface stability of the semiconductor layer,[17] the formation of an insulator layer between the metal and the semiconductor interface and R_S of devices are effective in the performance of these diodes.[13] However, traditional ways of oxidation and also deposition processes on the insulator layer of Si substrates still contain problems in passivation of the active dangling bonds at the semiconductor surface.[13] In this approach, the interfacial insulator layer, silicon-dioxide (SiO_2), is a novel material and tin-dioxide (SnO_2) and titanium-dioxide (TiO_2) also gain importance as potential materials in such applications.[18–21] Alternatively, the nitridation of silicon films is being examined for surface passivation in replacing SiO_2. Here, the silicon nitride (Si_3N_4) film layer is expected to suppress both the leak current in insulating gate materials and the interface reaction with metal oxides with a low density of surface states and high dielectric permittivity.[4,17] The electronic properties of Si_3N_4, such as high dielectric constant and larger energy gap,[11,12] motivate applications for the fabrication of device structures.[3]

In an ideal case, the current transport mechanism under applied bias voltage is expected to be a pure thermionic emission (TE), in which free charge carriers can gain enough energy to surmount the potential barrier with temperature (T). However, in the analysis of Schottky diodes, abnormal behaviors, such as the decrease in barrier height (BH) and increase in ideality factor (n) with decreasing T, and also the nonlinearity of the Richardson plot in the working T region can be observed in experimental $I-V$ relationships. Among them, the origin of these variations in BH and n under the effect of T can be modeled by using the TE mechanism together with the assumption of a Gaussian distribution (GD) of BHs. Although the current transport mechanism in MS or MIS Schottky barrier diodes (SBDs) are mainly expressed by TE theory, the existence of an insulator layer at the interface can affect the origin of the dominant mechanism. Therefore, experimental studies of diode parameters have been characterized by different transport models. Among them, in order to explain such abnormal deviations from the ideal TE model, discrete low-barrier regions are mostly assumed to be effective in a uniform BH formation on the basis of a TE mechanism with the GD of BH.

In the literature, several works have reported on various metals used for the formation of Schottky contacts on 4H-SiC[22–29] and MIS Schottky diodes.[3,13,17] Based on this research, the possible current conduction mechanism and device parameters such as n, Φ_{B0}, R_S, D_{it} in Au/Si_3N_4/4H n-SiC MIS diodes were analyzed by $I-V$, $C-V$ and $G/\omega-V$ measurements under the T range of 160–400 K.

EXPERIMENTAL

A single-crystalline semiconductor (0001) 4H-SiC wafer with donor concentration of 3.1×10^{16} cm^{-3} and about 500 μm thickness was used as a substrate material to fabricate the Au/Si_3N_4/4H n-SiC MIS diode. The wafer was cleaned by ultrasonic and chemical cleaning procedures in organic solvents ($CHClCCl_2$, CH_3COCH_3, and CH_3OH) for 10 min. After this cleaning process, the surface of the wafer was subjected to etching and then rinsing in deionized water with around 18 MΩ.cm resistivity. In order to analyze the electrical characteristics of this MIS diode, an ohmic back contact for the SiC wafer was created by evaporating Au. In this thermal evaporation step, the substrate temperature, T_{sub} was kept at about 450°C, and a 200-nm-thick Au metal contact was evaporated under 10^{-7} mbar vacuum conditions. Then, to increase the ohmic behavior of this coating, post-annealing treatment was applied at 430°C under thae nitrogen atmosphere. Next, a 5-nm-thick Si_3N_4 thin film layer was deposited by a metal–organic chemical vapor deposition (MOCVD) system.[30] To get a better understanding of the surface morphology of the Si_3N_4 layer, atomic force microscopy (AFM) was carried out in tapping mode. As shown in Fig. 1, the surface of the Si_3N_4 thin film was observed to have smooth and uniform characteristics. From this analysis, the root mean square roughness of Si_3N_4 was found to be 0.288 nm. Finally, the MIS diode structure was completed with thermally evaporated dot-patterned Au rectifying contacts, of 2 mm diameter and 150 nm thickness, on the front surface of the Si_3N_4 film layer.

The diode characteristics were analyzed by T-dependent $I-V$, and $C-V$ and $G/\omega-V$

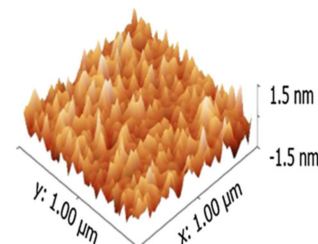

Fig. 1. AFM image of Si_3N_4 thin film layer.

measurements. A Keithley 2401 sourcemeter was used as a source/measure unit and the sample T was scanned from 160 K to 400 K with the help of a CTI-Cryogenics Model 22 refrigerator system combined with a Model SC helium compressor. In this measurement system, the T of the sample was controlled and arranged by using a Lakeshore DRC-91C controller. f-dependent $C-V$ and $G/\omega-V$ measurements were carried out with a computer-controlled system by using a Hewlett Packard 4192A LF model impedance analyzer.

RESULTS AND DISCUSSION

Current–Voltage Analysis

The fabricated Au/Si_3N_4/4H n-SiC MIS diode was analyzed under T-dependent $I-V$ measurements to determine the diode parameters and define the possible current transport mechanisms dominant in this structure. The experimental forward and reverse bias $I-V$ characteristics of the diode were investigated in the T range of 160–400 K, and the obtained $I-V$ plot is presented in Fig. 2. From this figure, the studied MIS structure shows a rectifying diode behavior that can be evaluated as an indication of a typical Schottky junction diode.[6] The forward currents of the diode increase with increasing T , and this variation was also observed in the reverse bias region. The rectification ratio defined as a ratio of forward to reverse currents at a constant voltage was calculated in about three orders of magnitude. In the ideal case, pure TE is expected to be the dominant current transport mechanism in the SBDs and the diode parameters are derived from this theory from the $I-V$ measurements.[6] However, in the experimental case of $I-V$ characteristics, SBDs generally show deviations from the ideal TE model. In this case, n can be take a value different from unity and is expected to be introduced to express this deviation. Thus, the real $I-V$ characteristics of the fabricated SBDs can be evaluated by inserting a parameter n to the expression of current through the junction barrier in the forward bias region as,

$$I = I_0\left[\exp\left(\frac{qV}{nkT}\right) - 1\right] \quad (1)$$

where I_0 is the reverse-saturation current, q is the electronic charge, V is the voltage value in the forward bias region, k is the Boltzmann constant and T is the ambient T (in the unit of K) during the measurement.

As given in Fig. 2, in the low bias voltage region, a semi-logarithmic $I-V$ relationship was found in the Shockley current–voltage characteristic; however, this curve deviates from linearity in the high bias voltage region. This observed non-linear I–V characteristics can mostly be attributed to the effects of the insulator layer between the metal and the semiconductor; D_{it}, R_S and the formation of

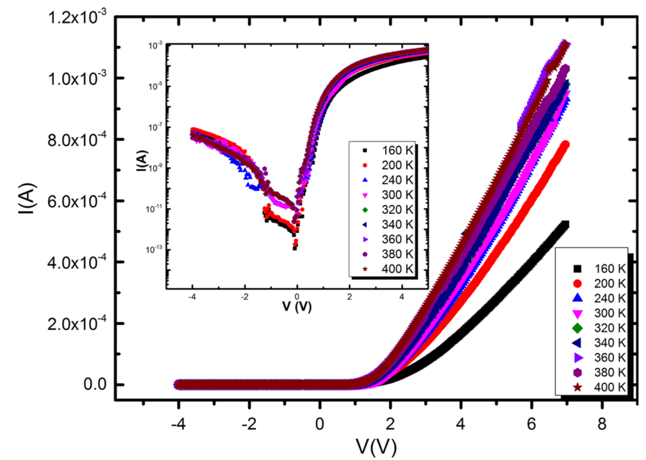

Fig. 2. $I-V$ characteristics of the MIS diode as a function of T. Semi-logarithmic $I-V$ plot, is shown in the inset.

BH.[21,29] In fact, this deviation in the electrical characteristics of SBDs with an interfacial insulator layer is expected in the applications by using SiO_2, SnO_2 and Si_3N_4 layers.[19]

From Eq. 1, I_0 is evaluated from the straight-line intercept of the $\ln I-V$ curve in the forward bias region and the experimental values are found at the zero bias voltage point as,

$$I_0 = AA^*T^2\exp(-q\Phi_{B0}/kT) \quad (2)$$

where A is the effective diode area, A^* is the effective Richardson constant and Φ_{B0} is the BH at the zero bias point. According to the assumptions of the TE model by using Eq. 1, A^* can be described according to the nearly free electrons in vacuum as the following relationship,

$$A^* = 4\pi m^*k^2/h^3 = 120(m^*/m) \quad (3)$$

with Planck constant, h, the mass of the majority carrier m and its constant effective mass value m^*.[31] This parameter has been reported as 146 A/cm^2 K^2 for the 4H n-SiC compound.[32,33] Additionally, by using the modified I–V relationship given in Eq. 1, the ideality factor n can be obtained from the slope of the linear region of $\ln I-V$ curve as,

$$n = \frac{q}{kT}\left(\frac{dV}{d\ln(I)}\right) \quad (4)$$

According to Eq. 2, the results were found in the range of 2.50–6.94 depending on ambient T , and they are also given in Table I, with the values being higher than unity and in decreasing behavior with the increase in T. High values of n can be attributed to the presence of interface states at the junction and barrier inhomogeneities with low barrier patches.[34,35] Since this is an indication of the quality of the fabricated junction together with R_S, and also the current flow mechanism in the

Table I. Diode parameters calculated according to the TE model

T (K)	*n*	Φ_{B0} (eV)
160	6.94	0.37
200	5.26	0.56
240	4.23	0.68
300	3.24	0.84
320	2.98	0.87
340	2.68	0.93
360	2.64	0.94
380	2.54	0.97
400	2.50	0.98

junction, the alternative possible models can be applied to define the dominant transport mechanism.

By using the theoretical approach, Φ_{B0} can be obtained from the I_0 values as,

$$\Phi_{B0} = \frac{kT}{q}\ln\left(\frac{AA^*T^2}{I_0}\right) \tag{5}$$

In this calculation (Eq. 5), experimental Φ_{B0} values were estimated at each T according to the Richardson constant of the 4H n-SiC layer.[32,33] The calculated values are listed in Table I and were found in increasing behavior with the increase in T, which is because the number of carriers having enough energy to surmount the barriers increased and contributed to the conduction with increasing T.[36] On the other hand, in the low T case, electrons can possibly pass over the lower barriers. Therefore, the current flow at the junction can be dominated through patches of the lower SBH.[37,38]

T-dependence of Φ_{B0} , and n can be seen as the consequence of a non-homogeneous BH formation in the junction. In fact, the deviation from ideality with high n values is expressed as a laterally inhomogeneous diode structure.[39] This approximation was evaluated by an examination of the degree of BH variation under the consideration of Tung's model and the linearity of the relationship between Φ_{B0} and n.[40] As seen in Fig. 3, these values were found to be inversely proportional to each other and the expected linear behavior was also obtained. From the extrapolation of this linear correlation to $n = 1$, a laterally homogeneous BH value was found to be about 1.5 eV for this structure.[40,41] According to Tung's model, in the presence of SBH inhomogeneity, the existence of local non-uniform patches of relatively lower or higher barriers with respect to an average BH are considered.[42] The observed deviations from ideal I–V characteristics in the fabricated diode structure can be explained on the basis of a TE mechanism with a GD of BHs.[43,44] According to this model, an inhomogeneous SBH assuming an abnormal increase in Φ_{B0} and decrease in n with increasing T, T and bias-dependent BH is

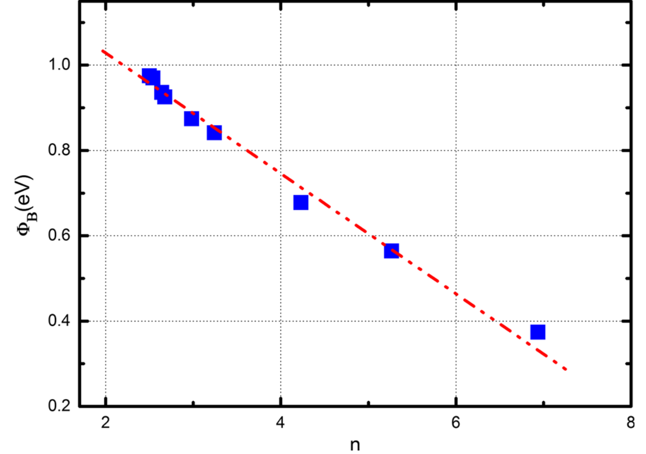

Fig. 3. Φ_{B0} versus n for the MIS diode.

described in terms of a Gaussian-type function.[44] It is modeled as there is an interaction between patches with different barriers and the effective barrier is expected to be lower than the mean value of the barrier distribution. Thus, many patches with different barriers are approximated around the mean BH.[5]

In this theory, the Gaussian function SBH is expressed with a mean value of BH ($\bar{\Phi}_B$) and a standard deviation (σ_S) as the following normalization distribution function giving the probability of accuracy for BH, $P(\Phi_B)$,

$$P(\Phi_B) = \frac{1}{\sigma_S\sqrt{2\pi}}\exp\left(-\frac{(\Phi_B - \bar{\Phi}_B)^2}{2\sigma_S^2}\right) \tag{6}$$

where the pre-exponential term, $1/\sigma_S\sqrt{2\pi}$, is the normalization constant of GD. Then, the total current through the junction with the contributions of the current flows at all spatial patches having different BH can be evaluated according to this probability of the occurrence of BH Φ_B as

$$I(V) = \int_{-\infty}^{\infty} I(\emptyset_b, V)P(\emptyset_b)\mathrm{d}V \tag{7}$$

where $I(\Phi_B, V)$ is a current at a bias V forΦ_B.[5,17] In this integral expression, the total current $I(V)$ through the SBH at a forward bias voltage is estimated as a summation of the current flows, and therefore it can be obtained by performing integration from $-\infty$ to $+\infty$.

Resulting from the non-ideal junction behavior, the modified I–V relationship can be described as,

$$I(V) = AA^*T^2\exp\left[-\frac{q}{kT}\left(\bar{\Phi}_B - \frac{q\sigma_S^2}{2kT}\right)\right] \exp\left(\frac{qV}{n_{ap}kT}\right)\left[1 - \exp\left(-\frac{qV}{kT}\right)\right] \tag{8}$$

with

$$I_0 = AA^*T^2\exp(-q\Phi_{ap}/kT) \quad (9)$$

where Φ_{ap} and n_{ap} are the apparent BH and the ideality factor, respectively.

Additionally, using the assumption of the GD, the BH can be described[45,46]

$$\Phi_{ap} = \bar{\Phi}_{B0}(T=0) - \frac{q\sigma_0^2}{2kT} \quad (10)$$

where $\bar{\Phi}_{B0}(T=0)$ is the mean SBH at zero bias ($V=0$) and extrapolated towards zero T, σ_0 is the standard deviation at zero bias. From the relationship between Φ_{ap} and $q/2kT$ as seen Fig. 4, the straight line behavior yields $\bar{\Phi}_{B0}$ and σ_0 from the intercept and slope, respectively. In this analysis, σ_0 was calculated as 0.169 and this lower value can be associated with the rectifying performance of the diode with barrier homogeneity. Since it is a measure of homogeneity in the barrier formation, this value of σ_0 corresponds to a more homogeneous BH or patches at around Φ_{B0}.[13] Furthermore, as compared to the calculated value, 1.40 eV, this deviation is 12% of $\bar{\Phi}_{B0}$ and therefore the interface inhomogeneties should be discussed in this diode structure.[24] $\bar{\Phi}_{B0}$ approximated by the GD model is also greater than the value of the uniform SBH found by using Tung's theory.

With the deviation from the ideal case, the voltage effect in n values can be formulated by the bias-dependent Gaussian coefficients as,

$$\left(\frac{1}{n_{ap}} - 1\right) = -\rho_2 + \frac{q\rho_3}{2kT} \quad (11)$$

ρ_2 and ρ_3 are bias voltage coefficients and measure the voltage deformation of the BH distribution.[45,47] It is assumed that the mean SBH ($\bar{\Phi}_B$) and σ_S are linearly bias-dependent on Gaussian parameters such that $\Phi_B = \bar{\Phi}_{B0} + \rho_2 V$ and standard deviation $\sigma_S = \sigma_{S0} + \rho_3 V$.[29,48] The corresponding $(n^{-1}-1)$ versus $q/2kT$ plot is given in Fig. 5, and the obtained straight line was analyzed to determine these voltage coefficients from the intercept and slope as $\rho_2 = 0.013$ and $\rho_3 = 0.423$. The linearity in Fig. 5 shows that n is the indication of the voltage deformation of the GD of the BH. In addition, the experimental results obtained from the analysis in both Eqs. 10 and 11 show the presence of a single GD of BH.[48]

Under GD approximation in the SBH of this diode, the Richardson equation should be modified from the pure TE model. In the real case, the Richardson constant can be extracted from Eq. 2 by plotting $\ln(I_0/T^2)$ as a function of inverse T $(1/T)$. However, according to the modified I–V relationship based on the barrier inhomogeneity, this expression should be re-evaluated by combining Eqs. 9 and 10, and the plot should give a linear relationship. Thus, the Richardson plot can be modified as follows,

$$\left(\frac{I_0}{T^2}\right) - \left(\frac{q^2\sigma_S^2}{2k^2T^2}\right) = \ln(AA^*) - \frac{q\bar{\Phi}_{B0}}{kT} \quad (12)$$

From Eq. 12, the obtained $\ln(I_0/T^2) - (q^2\sigma_0^2)/(2k^2T^2)$ versus q/kT plot is illustrated in Fig. 6. With a straight line behavior, the modified Richardson plot was analyzed in which the slope of the line corresponds to $\bar{\Phi}_{B0}$ and the extrapolation value was used to determine A^* for a given diode area, A. The calculated mean zero-bias value from this expression was 1.53 eV and can be accepted as a close approximation to the value found from the apparent BH versus $q/2kT$ curve of the Au/Si$_3$N$_4$/4H n-SiC diode (Fig. 4). Moreover, the Richardson constant A^* of this diode was in a close agreement the literature,[32,33] as 137.21 A/cm^2 K^2.

The deviations from ideality in the semi-logarithmic plot of forward bias I–V characteristics (Fig. 2) can be principally related to the effect of R_S. The

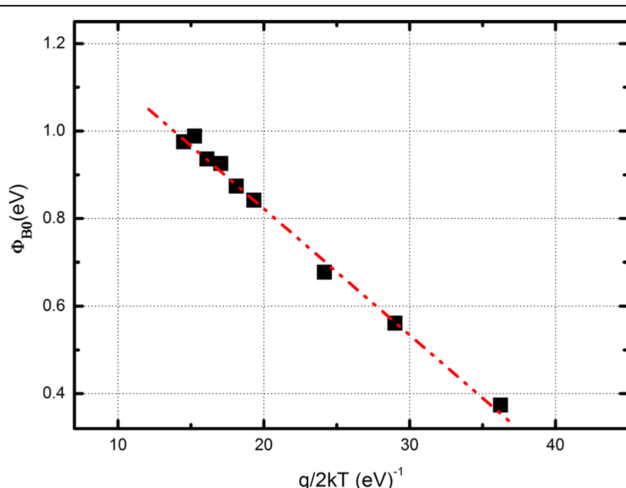

Fig. 4. Φ_{B0} versus $q/2kT$ curve of the MIS diode.

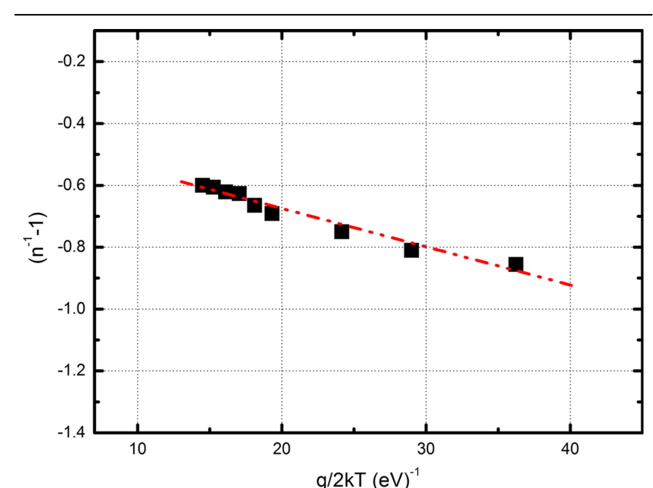

Fig. 5. $(n^{-1}-1)$ versus $q/2kT$ curve of the MIS diode.

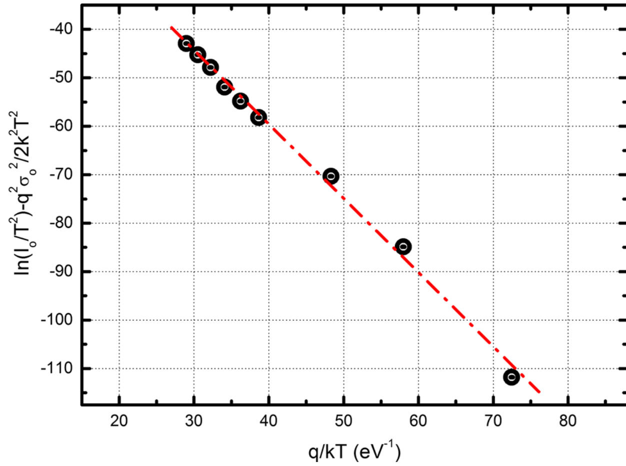

Fig. 6. $\ln(I_0/T^2) - (q^2\sigma_0^2)/(2k^2T^2)$ versus q/kT of the MIS diode.

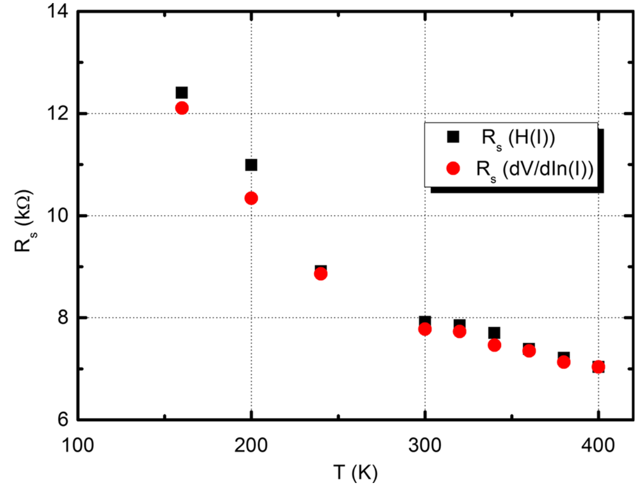

Fig. 7. Plot of T -dependent R_S values for the MIS diode.

resistance in the diode in the direction of the current flow was evaluated according to the method of Sato and Yasumura[49] and Cheung and Cheung,[50] as

$$\frac{\mathrm{d}V}{\mathrm{d}(\ln I)} = IR_S + n\left(\frac{kT}{q}\right) \quad (13)$$

and

$$H(I) = V - n\left(\frac{kT}{q}\right)\ln\left(\frac{I}{AA^*T^2}\right) = n\Phi_{B0} + IR_S \quad (14)$$

In these relationships given in Eqs. 13 and 14, T -dependence of the values of $R_S T$ were approximated with the TE theory at the high forward bias region.[6] From the slope of these plots, the values of R_S were obtained and are presented in Fig. 7, in which the calculated R_S values from these two linear relationships are in a good agreement with each other. The decrease in the resistance values with increasing T can be explained by the increase of the ideality factor n and the lack of free carrier concentrations at low T.[51]

Capacitance–Voltage Analysis

The C–V and G/ω–V measurements were carried out as a function of both f and T and are presented in Figs. 8 and 9, respectively. In order to investigate the f - and T -dependence of the Au/Si_3N_4/4H n-SiC MIS diode, these measurements were carried out in the temperature range of 160–400 K and in the f range of 10–1000 kHz.

In the case of the ideal C–V behavior of the Schottky diode, it is expected to be independent of the variation in applied f and the increase in capacitance with increasing forward bias voltage.[6] However, as expected from the literature on MIS Schottky diodes, the C–V characteristics of the fabricated diode give an anomalous capacitance peak at a certain bias voltage in each T step, and they were observed as in reverse shift with increasing T.[52–54] These characteristics can be related to the effect of R_S and the presence of interface states. On the other hand, this peak value of the capacitance is in decreasing behavior with increasing f and it exhibits the effect of interface properties in the diode structure, such that the interface states respond differently to low and high frequencies.[52] As shown in Fig. 8b, the interface states seem to follow the AC signal at low f and, with the contribution of capacitance of the interface states, the total capacitance of the diode was observed in increasing behavior. However, the decrease in capacitance with increasing f occurs because, at high f values, they cannot follow the AC signal and therefore the contribution of the interface state capacitance to the total capacitance is negligibly small.

In Fig. 9, the variation of G/ω with respect to the applied bias voltage depending on ambient f and T is illustrated and, as in the results of C–V measurement, a non-ideal behavior was observed with the effect of the characteristics of an inhomogeneous barrier. Similarly, applying a small AC signal causes a decrease in conductance due to the switching of the majority carriers between the majority carrier band of the semiconductor and interface states.[55]

In order to find the D_{it} values, it is possible to analyze the C–V and G/ω–V results according to the Hill–Coleman method.[56] Therefore, it was applied to determine the f -dependence distribution of D_{it} values obtained by the following relationship;

$$D_{it} = \left(\frac{2}{qA}\right)\frac{(G_m/\omega)_{max}}{\left((G_m/\omega)_{max}/C_i\right)^2 + (1 - C_m/C_i)^2} \quad (15)$$

where ω is the angular f, the values of C_m and G_m correspond to the measured capacitance and conductance values, respectively, and $(G_m/\omega)_{max}$ is the peak value, and the term C_i is the capacitance of the

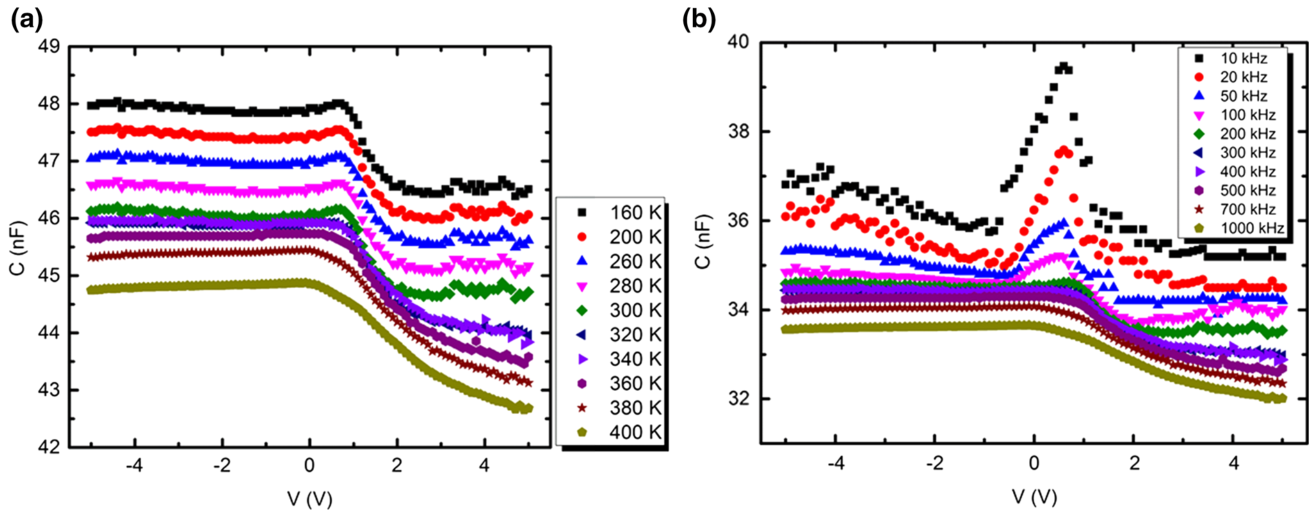

Fig. 8. (a) T - and (b) f -dependent $C-V$ characteristics of the MIS diode.

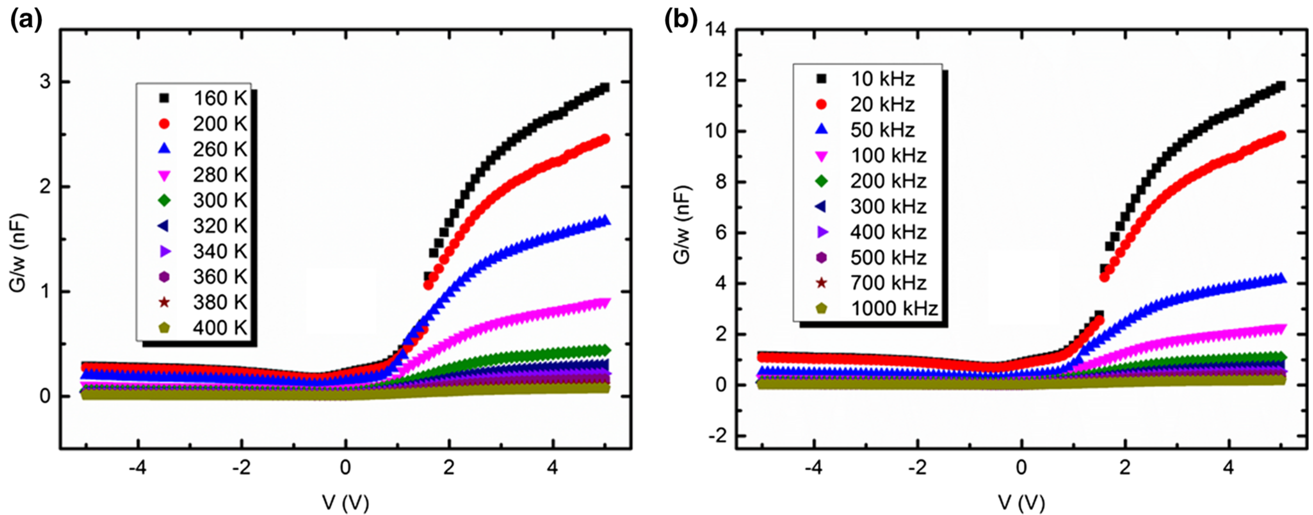

Fig. 9. (a) T - and (b) f -dependent $G/\omega-V$ characteristics of the MIS diode.

insulator layer. The results obtained according to Hill–Coleman method are plotted in Fig. 10. Since the capacitance and conductance are quite sensitive at both low T and low f regions, the values of D_{it} were observed in decreasing behavior as a function of these two variables.

For MIS-type diodes, the forward bias $I-V$ results can be used to determine the D_{it} values by considering the interface states in equilibrium with the semiconductor.[57] This behavior can be expressed as the voltage-dependent ideality factor in which the values of n are greater than unity,

$$n(V) = 1 + \frac{\delta}{\varepsilon_i}\left(\frac{\varepsilon_s}{w_D} + qD_{it}\right) \tag{16}$$

where δ is the thickness of the interfacial layer, w_D is the width of the space charge region, and ε_i and ε_s are the permittivity of interfacial insulator and semiconductor layers, respectively.[58,59] By using Eq. 16, the density distribution profiles of D_{it} were obtained as a function of $E_{SS}-E_V$ values (Fig. 11). In this energy parameter, E_{SS} is defined as the energy of the interface states from the top of the valence band at the semiconductor surface, and it is given by,

$$E_{SS} - E_V = q(\Phi_e - V) \tag{17}$$

with Φ_e and exhibits a voltage-dependent parameter with the possibility of an interface state in the diode.[58]

As seen in Fig. 11, the experimental values of interface state density were in decreasing behavior with increasing T. This T -dependent variation can be observed due to the restructuring and the reordering of the interface layer under the effect of T.[56,59]

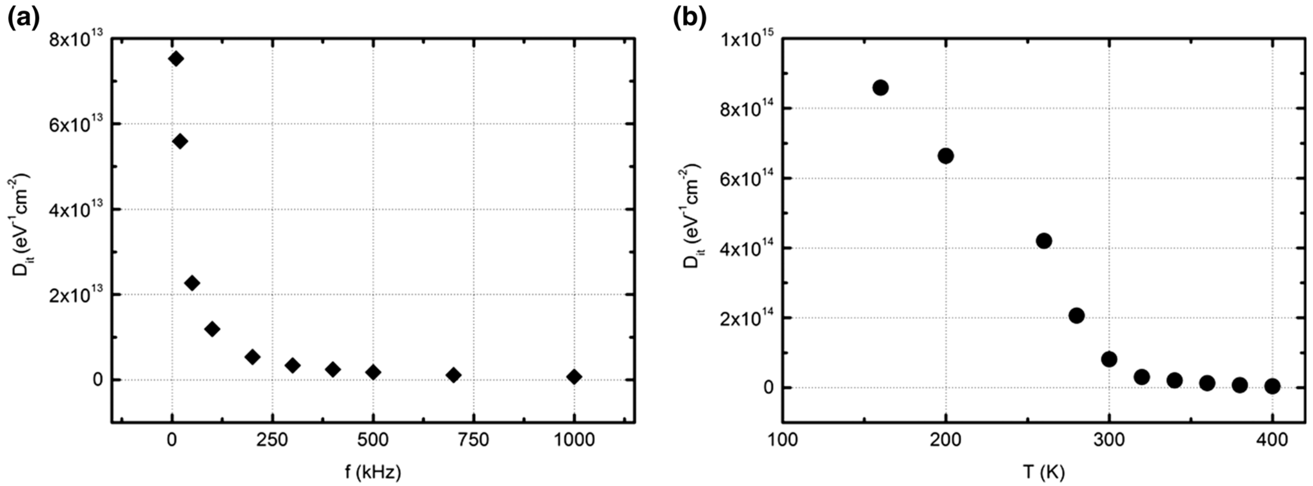

Fig. 10. The variation of D_{it} as a function of (a) f and (b) T.

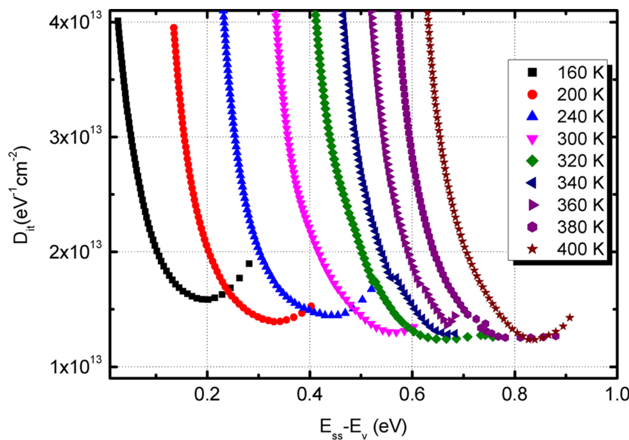

Fig. 11. Plot of D_{it} versus $E_{SS}-E_V$ resulting from the $I-V$ measurements.

CONCLUSION

In the present work, a Au/Si_3N_4/4H n-SiC MIS diode was fabricated and its electrical properties were investigated under T -dependent $I-V$; and f - and T -dependent $C-V$ and $G/\omega-V$ measurements. The forward I–V behavior of the diode was modeled by TE theory with a GD of BH due to the effect in inhomogeneous BH at the interface. $\bar{\Phi}_{B0}$ and σ_S were found to be 1.43 eV and 0.169 eV, respectively. Based on the inhomogeneity of the BHs, the corrected value of the Richardson constant was calculated as 141.648 A/cm^2 K^2. In addition, the T -dependence of the values of R_S were determined using Cheung's model and R_S was found in decreasing with increasing TR_S. $C-V$, and $G/\omega-V$ plots indicated that the capacitance and conductance values are only sensitive at high T and low f regions. This result was confirmed by possible restructuring and re-ordering of the interface under a thermal effect. The effect of the capacitance of the insulator layer was evaluated by the Hill–Coleman method and D_{it} were calculated depending on the variations in both f and T.

ACKNOWLEDGEMENTS

This work was partially supported by The Management Unit of Scientific Research Project of Hitit University under Grant Nos. FEF19002.15.001 and FEF19004.15.010.

REFERENCES

1. C.G.V. Walle, *Wide-Band-Gap Semiconductors* (Amsterdam: North-Holland, 1993).
2. C.Y. Chang, F.M. Pan, J.S. Lin, T.Y. Yu, Y.M. Li, and C.Y. Chen, *J. Appl. Phys.* 120, 234501 (2016).
3. F.Z. Pür and A. Tataroğlu, *Phys. Scr.* 86, 035802 (2012).
4. S. Zeyrek, Ş. Altındal, H. Yuzer, and M.M. Bülbül, *Appl. Surf. Sci.* 252, 2999 (2006).
5. A. Tataroğlu and F.Z. Pür, *Phys. Scr.* 88, 015801 (2013).
6. S.M. Sze and K.K. Ng, *Physics of Semiconductor Devices* (Hoboken: Wiley, 2007).
7. I.R. Kaufmann, A. Pick, M.B. Pereira, and H.I. Boudinov, *Semicond. Sci. Technol.* 30, 125002 (2015).
8. G.S. Chung, K.S. Kim, and F. Yakuphanoglu, *J. Alloys Compd.* 507, 508 (2010).
9. N. Yıldırım, A. Turut, and V. Turut, *Microelectron. Eng.* 87, 2225 (2010).
10. P.G. Neudeck, *J. Electron. Mater.* 24, 283 (1995).
11. K.J. Schoen, J.M. Woodall, J.A. Cooper Jr., and M.R. Melloch, *IEEE Trans. Electron. Devices* 45, 1595 (1998).
12. Q. Wang, X. Cheng, L. Zheng, P. Ye, M. Li, L. Shen, J. Li, D. Zhang, Z. Gu, and Y. Yu, *Appl. Surf. Sci.* 409, 71 (2017).
13. S. Alialy, Ş. Altındal, E.E. Tanrıkulu, and D.E. Yıldız, *J. Appl. Phys.* 116, 083709 (2014).
14. J.B. Casady and R.W. Johnson, *Solid State Electron.* 39, 1409 (1996).
15. R. Singh, J.A. Cooper, M.R. Melloch, T.P. Chow, and J.W. Palmour, *IEEE Trans. Electron. Devices* 49, 665 (2002).
16. M. Sochacki, A. Kolendo, J. Szmidt, and A. Werbowy, *Solid State Elctron.* 49, 585 (2005).
17. M.M. Bülbül, S. Zeyrek, Ş. Altındal, and H. Yüzer, *Microelectron. Eng.* 83, 577 (2006).
18. R.S. Dale, C.S. Rastomjee, F.H. Potter, R.G. Egdell, and T.J. Tate, *Appl. Surf. Sci.* 70, 359 (1993).
19. M. Özer, D.E. Yıldız, Ş. Altındal, and M.M. Bülbül, *Solid State Electron.* 51, 941 (2007).

20. Ş. Altındal, S. Karadeniz, N. Tuğluoğlu, and A. Tataroğlu, *Solid State Electron.* 47, 1847 (2003).
21. A. Tataroğlu, Ş. Altındal, and M.M. Bülbül, *Microelectron. Eng.* 81, 140 (2005).
22. İ. Taşçıoğlu, Ö.T. Özmen, H.M. Şağban, E. Yağlıoğlu, and Ş. Altındal, *J. Electron. Mater.* 46, 2379 (2017).
23. R. Yakimova, C. Hemmingsson, M.F. Macmillan, T. Yakimov, and E. Janzén, *J. Electron. Mater.* 27, 871 (1998).
24. S. Toumi, A. Ferhat-Hamida, L. Boussouar, A. Sellai, Z. Ouennoughi, and H. Ryssel, *Microelectron. Eng.* 86, 303 (2009).
25. L. Boussouar, Z. Ouennoughi, N. Rouag, A. Sellai, R. Weiss, and H. Ryssel, *Microelectron. Eng.* 88, 969 (2011).
26. R. Weiss, L. Frey, and H. Ryssel, *Appl. Surf. Sci.* 184, 413 (2001).
27. F. Roccaforte, F. La Via, V. Raineri, R. Pierobon, and E. Zanoni, *J. Appl. Phys.* 93, 9137 (2003).
28. M.R. Aydın, N. Yıldırım, and A. Türüt, *J. Appl. Phys.* 102, 043701 (2007).
29. S. Alialy, Ş. Altındal, E.E. Tanrıkulu, and D.E. Yıldız, *J. Appl. Phys.* 116, 083709 (2014).
30. P.A. Yunin, Yu.N. Drozdov, M.N. Drozdov, S.A. Korolev, A.I. Okhapkin, O.I. Khrykin, and V.I. Shaskin, *Semiconductors* 49, 1421 (2005).
31. C.R. Crowell, *Solid State Electron.* 8, 395 (1965).
32. A. Itoh and H. Matsunami, *Crit. Rev. Solid State Mater. Sci.* 22, 111 (1997).
33. A. Itoh, T. Kimoto, and H. Matsunami, *IEEE Electron. Device Lett.* 16, 280 (1995).
34. H. Altuntaş, Ş. Altındal, H. Shtrikman, and S. Özçelik, *Microelectron. Reliab.* 49, 904 (2009).
35. A. Tataroğlu, *Phys. Scr.* 88, 015801 (2013).
36. V. Janardhanam, H. Lee, K. Shim, H. Hong, S. Lee, K. Ahn, and C. Choi, *J. Alloys Compd.* 504, 146 (2010).
37. H.C. Card and E.H. Rhoderick, *J. Phys. D Appl. Phys.* 4, 1589 (1971).
38. P. Chattopadhyay and A.N. Daw, *Solid State Electron.* 29, 555 (1986).
39. R.F. Schmitsdorf, T.U. Kampen, and W. Mönch, *J. Vac. Sci. Technol. B* 15, 1221 (1997).
40. R.T. Tung, *Appl. Phys. Lett.* 58, 2821 (1991).
41. C.R. Crowell, *Solid State Electron.* 20, 171 (1977).
42. R.T. Tung, *Phys. Rev. B* 45, 13509 (1992).
43. D.E. Yıldız, Ş. Altındal, and H. Kanbur, *J. Appl. Phys.* 103, 124502 (2008).
44. J.H. Werner and H.H. Guttler, *J. Appl. Phys.* 69, 1522 (1991).
45. Ş. Altındal, S. Karadeniz, N. Tuğluoğlu, and A. Tataroğlu, *Solid State Electron.* 47, 1847 (2003).
46. A. Gümüş, A. Türüt, and N.J. Yalçın, *Appl. Phys.* 91, 245 (2002).
47. J.H. Werner and H.H. Güttler, *Phys. Scr.* T39, 258 (1991).
48. S. Karatas, Ş. Altındal, A. Türüt, and A. Özmen, *Appl. Surf. Sci.* 217, 250 (2003).
49. K.S.Y. Yasumura, *J. Appl. Phys.* 58, 3655 (1985).
50. S.K. Cheung and N.W. Cheung, *Appl. Phys. Lett.* 49, 85 (1986).
51. Ş. Altındal, H. Kanbur, D.E. Yıldız, and M. Parlak, *Appl. Surf. Sci.* 253, 5056 (2007).
52. B. Şahin, H. Çetin, and E. Ayyıldız, *Solid State Commun.* 135, 490 (2005).
53. P. Chattopadyay and B. Raychaudhuri, *Solid State Electron.* 35, 605 (1993).
54. P. Chattopadyay and S. Sanyal, *Appl. Surf. Sci.* 89, 205 (1995).
55. W. Mönch, *Electronic Properties of Semiconductor Interfaces* (Berlin: Springer, 2004).
56. W.A. Hill and C.C. Coleman, *Solid State Electron.* 23, 987 (1980).
57. S. Zeyrek, Ş. Altındal, H. Yüzer, and M.M. Bülbül, *Appl. Surf. Sci.* 252, 2999 (2006).
58. D.E. Yıldız and Ş. Altındal, *Microelectron. Eng.* 85, 289 (2008).
59. B. Akkal, Z. Benamara, A. Boudissa, N. Bachir Bouiadjra, M. Amrani, L. Bideux, and B. Gruzza, *Mater. Sci. Eng. B* 55, 162 (1998).